16th World Conference on Earthquake, 16WCEE 2017
Santiago Chile, January 9th to 13th 2017
Paper N° 3975
Registration Code: S-T1463236702

OVER TWENTY YEARS SEISMIC MONITORING EXPERIENCE OF CABLE-STAYED BRIDGE: LESSONS LEARNED ON STRUCTURAL ASSESSMENTS

D.M. Siringoringo(1), Y. Fujino(2)

(1) IAS Associate Professor, Institute of Advanced Sciences, Yokohama National University, dion@ynu.ac.jp
(2) Distinguished Professor, Institute of Advanced Sciences, Yokohama National University, fujino@ynu.ac.jp

Abstract

Instrumentation of many bridges in Japan, especially the long-span cable-supported ones play an important role in seismic performance evaluation. Since Japan is located on seismically active area, these permanent instrumentations provide high quality seismic records every time an earthquake occurs that allow us to investigate seismic performance of the structure. In this study, seismic monitoring experience and the related research on the Yokohama-Bay Bridge, a cable-stayed bridge in Yokohama, Japan is presented. The bridge with central span of 460 m and two side spans of 200 m each is densely instrumented with 85 arrays of accelerometers. Seismic responses from more than a hundred earthquakes have been recorded since 1990 until 2011 including major events such as the 2004 Chuetsu-Niigata Earthquake and the 2011 Great East-Japan Earthquake, notably the largest earthquake ever recorded on the bridge. The paper describes lessons learned from over twenty years experience on monitoring especially on the structural assessment based on analysis of monitoring data. The monitoring results have been used to evaluate structural performance especially the link-bearing connection—a seismic isolation device on different level of earthquake, the effect of structural modification and seismic retrofit on the characteristics of seismic response, and detecting the occurrence of unexpected events such as longitudinal slip-slip behavior of link- bearing connection, lateral pounding between tower and girder during large earthquake, and vehicle overturning incident.

Keywords: seismic response; seismic monitoring; cable-stayed bridge; structural assessment; system identification

1. Introduction

Developments in design and construction of long-span bridges have always involved sophisticated models, analysis and cutting edge technologies. Instrumentation for measurement and performance monitoring of uncertainties associated with these new models, analysis and technologies are necessary to ensure the correctness and efficacy of their applications. For these reasons, many of long-span bridges have been instrumented and continuously monitored since their construction completions. Moreover many long-span bridges in Japan have been constructed in the seismically active and strong wind areas, consequently structural behaviors during seismic and wind loadings become major concerns. Historically, Japanese bridge monitoring system put more emphasis on structural evaluation against extreme events. Monitoring data are utilized to verify design assumptions, update specifications, and facilitate the efficacy of vibration control system. Later, monitoring systems are also used to evaluate structural performance under various environment and loading conditions, and detect the possible structural deterioration over the age of structures [1].

One of such instrumented long-span bridges is the Yokohama-Bay Bridge, a cable-stayed bridge near Yokohama area in Kanagawa, Japan. In this paper, we present lessons learned from over twenty years experience on monitoring the bridge especially on the structural assessment based on analysis of monitoring data. The monitoring results have been used to evaluate structural performance especially the link-bearing connection—a seismic isolation device on different level of earthquake, the effect of structural modification and seismic retrofit on the characteristics of seismic response, and detecting the occurrence of unexpected events such as longitudinal slip-slip behavior of link- bearing connection and lateral pounding between tower and girder during large earthquake.

2. Description of Yokohama-Bay Bridge

The bridge investigated in this research is Yokohama-Bay Bridge, located at the entrance of Yokohama harbor. It is a vital part of the Yokohama-Tokyo bay-shore expressway (see Fig. 1). It is a continuous three-span cable-stayed bridge with the main girder consisting of a double-deck steel truss-box. The central span is 460m with side spans of 200m each. The upper and lower deck have 6 and 2 lanes, respectively, with the upper deck being part of the Yokohama Expressway Bay shore route and the lower deck a part of the national route. The lower deck was added later and completed before 2004 Chuetsu-Niigata earthquake. The bridge has two H-shaped towers of 172m height and 29.25m width with a welded monolithic section. Construction was completed in 1988 and the bridge was opened in September 1989.

Fig.1. Yokohama-Bay Bridge

3. Description of Seismic Design and Retrofit Concept

Earthquake resistance was one of the main concerns in the bridge design. Considering seismicity of the area, possible recurrence of a large earthquake such as the 1923 Great Kanto Earthquake, the weak ground condition, and the high center of gravity of the bridge; special seismic design measure was adopted. The measure includes the use of Link-Bearing Connections (LBC), namely the 10-m-long end-links at the end-piers (P1 and P4) and 2-m-long tower-links at the towers (P2 and P3), to accommodate girder longitudinal motion. The LBC system maintains long longitudinal fundamental period and allows the girder to be suspended from towers and piers [2, 3]. As a result, the effect of inertia force of superstructure on substructure during an earthquake can be minimized.

By lengthening the natural period the structure experiences smaller acceleration but larger displacement. Shorter LBCs at the tower function to restrict excessive longitudinal displacement that could occur during a large earthquake. The LBCs are made of steel and consist of a solid main body in the middle part and circular bearings at both ends. Inside the bearings, steel rods are placed through an inner ring and tightened by bolts to two circular steel plates located on both sides of the main body (Fig. 2). The LBC is designed as a tension link. The pin connections at both ends accommodate in-plane rotations that allow girder longitudinal movement as in a pendulum system.

The original design model describes LBCs as longitudinal hinge connections, and they are expected to function as such in any level of earthquake. This implies that relative displacement between pier and girder will have to be sufficiently large to ensure that high-frequency components of pier and tower vibration are not transferred to the girder. When such a condition is satisfied, inertia force from girder on the piers and towers is minimized, and the amount of moment force on the substructures can be significantly reduced. This will create an isolation effect commonly found in base-isolated bridges. The fundamental longitudinal mode that captures such link behavior is noted as the longitudinal *slip* mode. The finite-element model generates such a mode with period of 7.7sec [2, 3]. In transverse direction, the girder is suspended over the piers and towers. Girder transverse movements are restricted by wind shoes located on the pier–girder and tower–girder connections. A small gap exists between wind shoes and girder to accommodate small relative motion. Part of girder connections that face wind shoes are covered with side bearings with Teflon Polytetrafluoroethylene (PTFE) surface, whereas the surfaces of wind shoes are made of stainless steel. Both side bearings and wind shoes are designed to resist maximum transverse load of 27,654 and 48,346 kN for pier–girder and tower–girder connections, respectively [3].

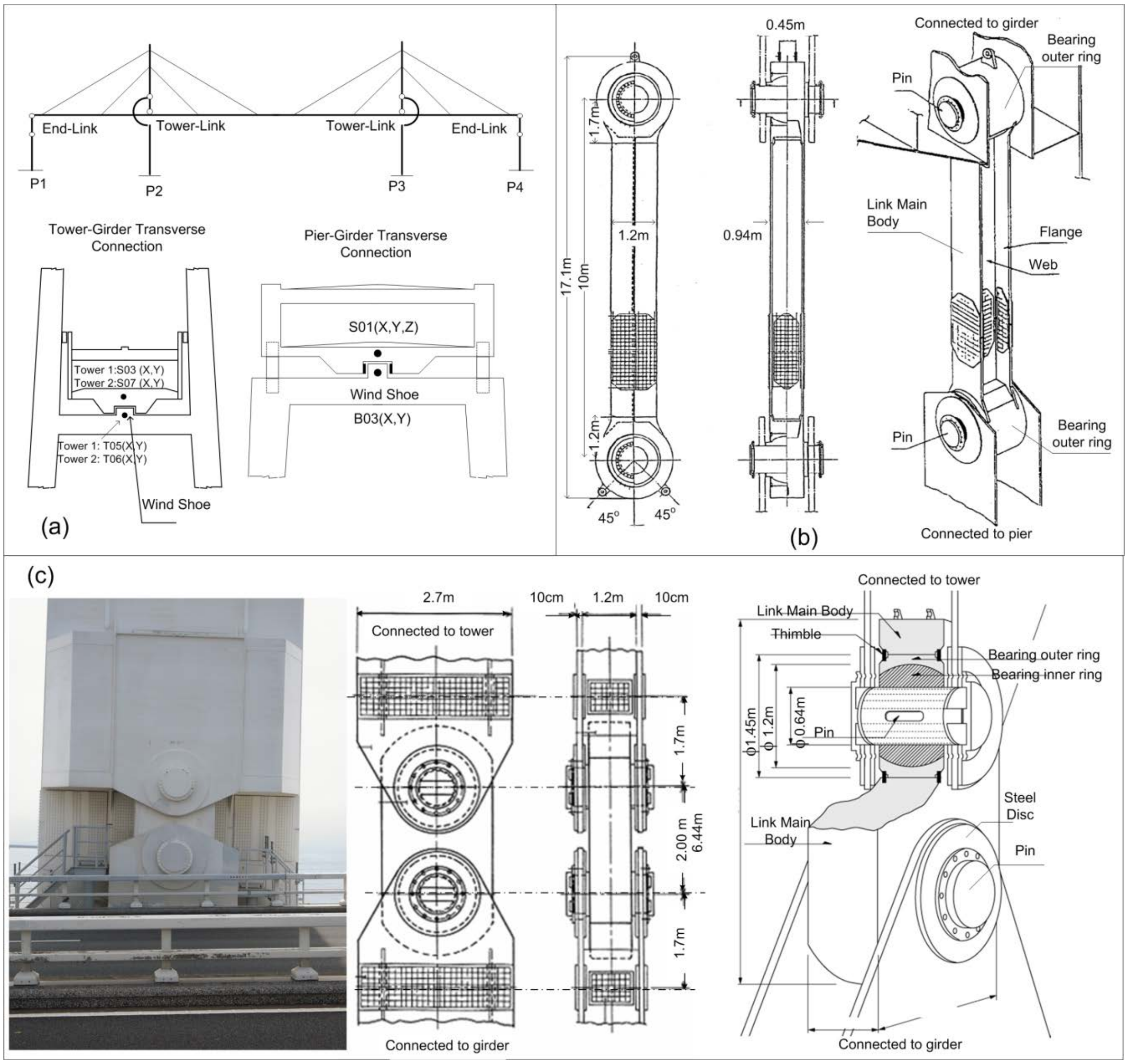

Fig.2. (a) Characteristics of pier–girder and tower–girder connections and location of sensors on the connections; (b) detail figure of end-link; (c) detail figure of tower-link. (After [4])

In 2005, a seismic retrofit program was conducted for safety assurance of a Level 2 earthquake according to Japan’s bridge seismic code. The retrofit program considered two types of maximum credible earthquakes: magnitude 8 far-field or moderately far-field large earthquakes taking place in the subduction zone of the Pacific plate with a near-field inland earthquake occurring beneath the site or close to the site. Based on the seismological model, the ground motions were simulated assuming seven scenarios with fault geometry that resembles the 1923 Great Kanto Earthquake [5]. Simulations identified potential damages for both types of ground motion and concluded that significant damage would occur on the towers and bearings under such excitations. Furthermore, the far-field ground motion would create more damage and induce 1.5-m longitudinal displacement of the girder. Accordingly, a fail-safe design concept was introduced, and the following strategies for major structural elements were implemented [5]:

1. Providing adequate seating on the approach span to avoid unseating during a large earthquake;
2. Constructing additional cables connecting girder and end-piers in case a large transverse excitation damages the two link-bearing connections (LBCs) at the end-piers;

3. Adding stiffeners inside the towers and piers to increase the ultimate strength and ductility in case a large longitudinal excitation damages the edge of steel frame;
4. Installing cable inside the lateral upper beam near top of the tower to prevent the beam from falling in case of a large deformation; and
5. Providing additional seats on the lateral beam under the girder to prevent impact force from girder in case a large transverse excitation damages the tower links and stay cables near the towers.

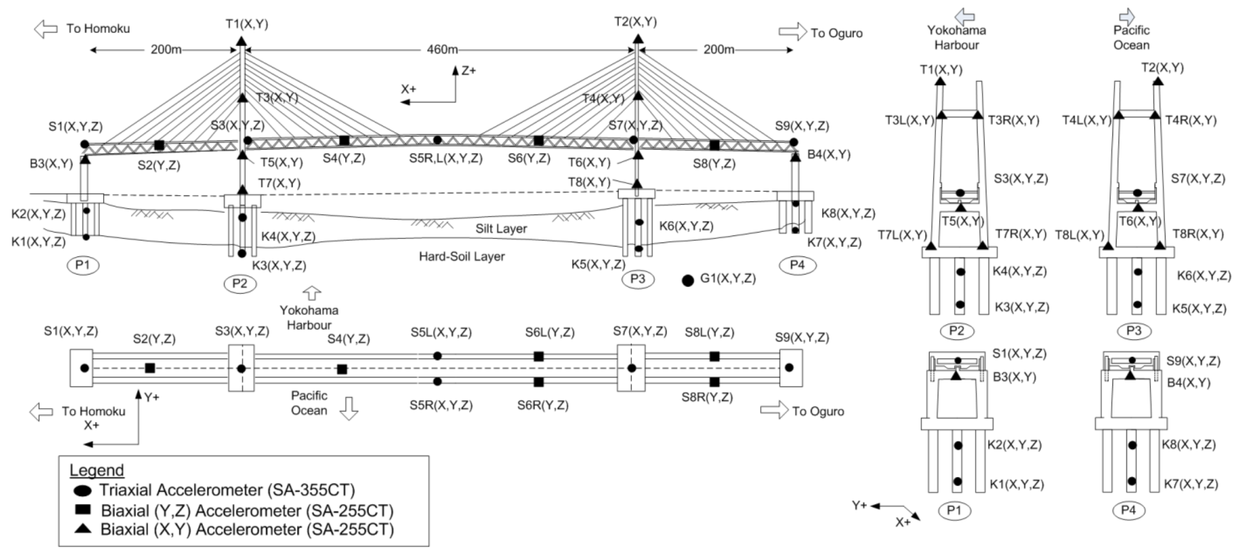

Fig.3. Seismic monitoring system of Yokohama-Bay Bridge

4. Description of Yokohama-Bay Bridge Monitoring System

The monitoring system of the Yokohama-Bay Bridge consists of 85 channels of permanently deployed sensors measuring acceleration responses at 36 locations in three directions. These accelerometers have a range of frequency between 0.05 and 35 Hz with an accuracy of 15 mA/cm/s^2. Among these 85 channels, 25 are located on the substructure (such as pile foundation and pile caps) and the rest are installed on the superstructure (towers, pier caps and girder). Along the girder, sensors were installed at 9 locations with a space of 115m between each. These sensors measure accelerations vertically, laterally (out-of-plane) and longitudinally (bridge axis). On one side of the bridge girder, starting from the Honmoku approach until the middle of the main span, accelerometers were installed only along one longitudinal axis of the bridge. On the other side, starting from the middle of the main span to the Daikoku approach, accelerometers were installed on both sides of the girder, thus providing adequate information for identification of torsional modes. Both towers are equipped with accelerometers measuring longitudinal and lateral movement at both of the bridge's H-shaped towers. This enables the identification of pure longitudinal, lateral and torsional modes. For end-piers, accelerometers were installed on the pile cap and pier cap. Using the response from the sensors on the pier cap and the girder just above the pier cap, one can observe the behavior of link-bearings connecting the girder with the towers and with the end-piers.

Two types of accelerometers are used: servo-type accelerometers SA-355CT (triaxial) and SA-255CT (biaxial) produced by manufacturer Tokyo Sokushin. These accelerometers have the maximum amplitude capability 20m/s^2, sensitivity 2m/s^2/V, and linearity 0.03% of the full scale. All sensors have frequency bandwidth of 0.05–35 Hz and operate at sampling frequency 100 Hz. The sensors are connected through a wired network system, and responses are recorded every time accelerations exceed the preset trigger level. The monitoring system is operated and maintained by Tokyo Metropolitan Expressway Public Corporation. Fig 3 illustrates sensor positioning and measuring direction.

5. Seismic Records from Long-term Monitoring system

The monitoring system was deployed after construction completion and started to record seismic responses of the structure from 1990. Seismic data presented in this paper is compilation of earthquakes recorded from January 1990 until April 2011, with the absence of records from 1998-2000, where at least 104 earthquakes have been recorded by the monitoring system. About half of the earthquakes are of significant level that is with intensity equal to or larger than 3 in the Japan Meteorological Agency's (JMA) scale. This implies ground motions whose the peak ground acceleration (PGA) at the bridge site (i.e. Yokohama station) is equal or more than equivalent to 0.08 m/s^2.

Table 1 shows the list of earthquakes recorded on the bridge along with the largest recorded earthquake in each year. One can observe that the largest ground motion ever recorded at the bridge is due to 2011 Great East Japan earthquake. Fig.4 shows the response spectra of free-field ground motions G1 located on the hard-rock layer about 100 m below the surface, along with the original design response spectrum for the hard rock layer and two seismic retrofit ground motions in 2005 that produce the largest acceleration spectra for period longer than 3 s. As shown in the figure, acceleration spectra of the main shock are smaller than both the original design and the retrofit.

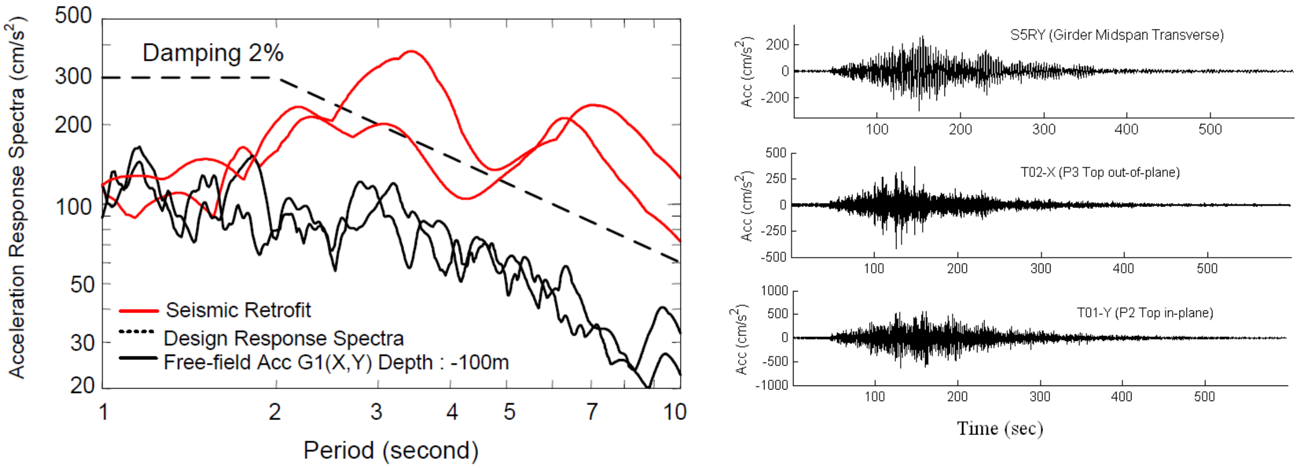

Fig.4. Acceleration response spectra at the free-field and the largest accelerations at the girder and top of the tower due to the 2011 Great East-Japan Earthquake, the largest ground motion ever recorded on the Yokohama-Bay Bridge

In the analysis the records were divided into the following groups: 1) earthquakes before 2004, which is before addition of new traffic lane on the lower deck, 2) earthquakes due to 2004 Chuetsu-Niigata and after, the 2004 Chuetsu Niigata earthquake generated main-shock and series of aftershocks, and 3) earthquakes due to 2011 Great East-Japan earthquake and aftershocks.

Of particular important events are the 2004 Chuetsu-Niigata and 2011 Great East-Japan earthquake. On the 23 October 2004 Chuetsu-Niigata area was hit by strong earthquake with magnitude Mw 6.8, two main shocks recorded at 17:57 and at 18:35, and followed by two aftershocks at the same day and the next day. This series of strong shaking were recorded at the bridge site and used to analyze bridge condition [7]. The seismic responses recorded from 2011 Great East-Japan earthquake consists of the March 9, 2011, foreshock; March 11, 2011, main shock at 14:47 JST; and nine aftershocks with JMA seismic intensity equal to or larger than 3 that occurred on March 11 and a few days after [4]. Seismic responses from the main shock last for about 10 min, the longest among the seismic data recorded.

6. System Identification and Structural Assessments

6.1 Data Analysis and Multi-Input Multi-Output System Identification applied to Seismic Responses

Table 1 – Recorded earthquakes on Yokohama-Bay Bridge from 1990 until 2011

Year	Number of Earthquake		The largest recorded earthquake in the year					
	Total	With intensity > 3 at bridge site	Date and Source or Name of Earthquake	Mw	JMA Intensity at bridge site	Distance from epicenter to bridge site (km)	Peak horizontal acc. at bridge footing (cm/s^2)	Peak vertical acc. at girder's midspan (cm/s^2)
1990	5	4	20-Feb Izu Oshima	6.5	4	92	18.45	47.91
1991	1	1	14-Jul Nagano-ken	5.4	3	150	5.75	15.65
1992	1	1	2-Feb Tokyo-Bay	5.9	3	27	19.09	43.42
1995	2	1	3-Jul Sagami-Bay	5.6	4	35	17.68	31.43
1996	2	2	11-Sept Chiba-ken Offshore	6.2	3	139	10.75	36.58
1997	2	2	9-Aug Saitama-ken Southern	4.7	3	44	9.05	23.03
2003	4	4	15-Oct Chiba-ken West	5.1	3	38.12	20.39	39.58
2004	6	4	23-Oct 2004 Chuetsu-Niigata	6.8	3	216.4	29.76	46.20
2005	17	10	23-Jul Northwest Chiba	6	5-	44.3	78.54	91.49
2006	11	7	2-May Izu Peninsula off coast	5.1	4	67.55	15.61	27.24
2007	7	2	16-Aug Chiba-ken East	5.3	3	77.53	3.5	22.31
2008	11	3	8-May Ibaraki-ken Off coast	7	3	194.2	10.1	40.76
2009	9	5	11-Aug Suruga-Bay	6.5	4	130.3	22.39	44.21
2010	6	1	30-Nov Ogasawara Islands	7.1	3	789.2	4.56	38.33
2011	24	7	11 March 2011 Great East Japan	9	5+	398	83.32	194.25

In general, the bridge superstructure responses were characterized by significant transverse vibration. The girder maximum acceleration was recorded in transverse direction. For the case of 2011 Great East-Japan earthquake for example, the maximum girder displacement of more than 60cm recorded in the middle of center-span in transverse direction. In general, the girder large vibration is mainly due to one mode that is the first girder transverse mode at 0.28-0.32Hz. Meanwhile, the girder vertical vibration is dominated by more modes between 0.32Hz and 1.2Hz [4]. Frequency characteristics can be obtained from spectra analysis and the results are confirmed by system identification. The spectra analysis is mostly adequate to provide quick observation of bridge response for small and moderate earthquakes. However, for large excitation as in the case of 2011 Great East-Japan earthquake, bridge responses may enter non-linear region, thus frequency spectra of the overall responses may not be adequate to represent time variation of the natural frequencies. Therefore, a time-frequency analysis by wavelet transform should be conducted [4].

Multiple-input multiple output (MIMO) system identification was used to evaluate fundamental vibration modes pertinent to the bridge seismic responses. The identification is based on the System Realization using Information Matrix (SRIM) [6] algorithm that utilizes correlations between input-output data to estimate modal parameters of dynamical system through a realization process. The identification procedure starts by estimating the observability matrix from the so-called information-matrix that is composed by correlation functions of input and output data. To implement the identification, one needs to select a set of input-output data. In this study responses from triaxial accelerometers located at the bottom of the end-pier (P1: sensor K2) and the towers (P2: sensor K4 and P3: sensor K6) were selected as inputs. These responses were utilized instead of the free-field responses (G1) to minimize the effect of soil-structure interaction and to realize the multi-input multi-output system. Unfortunately, during the 2011 Great East-Japan earthquake sensors at the bottom of P4 failed so they were not included in the analysis for seismic records in 2011. Since the inputs and outputs data are derived from multiaxial accelerations, the identification yields in three-dimensional mode shapes as shown in Fig.5.

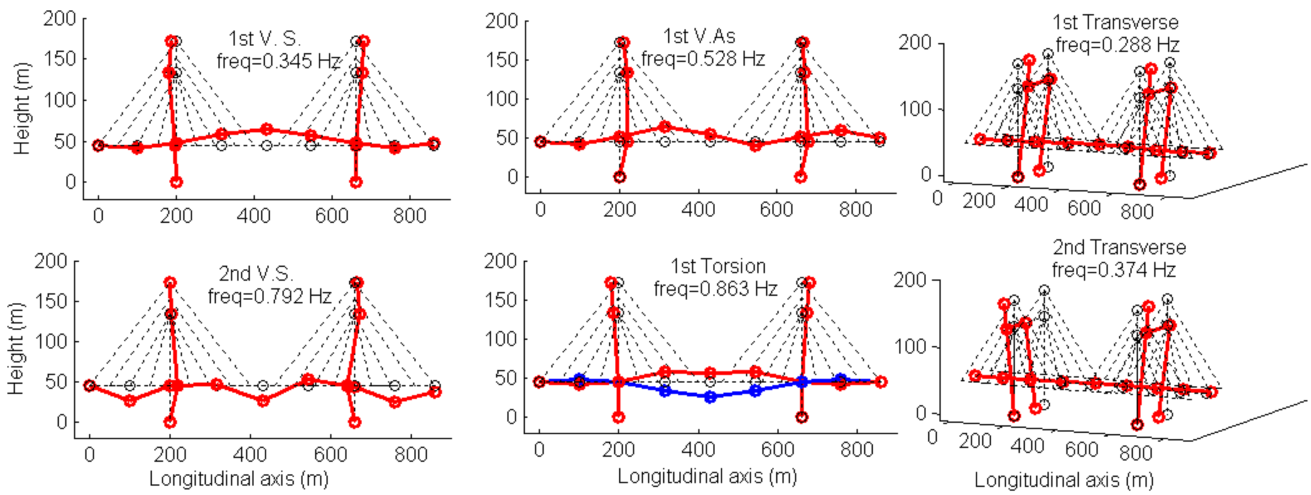

Fig.5. Example of mode-shapes identified from seismic response due to 2004 Chuetsu-Niigata earthquake

It should be mentioned that the system identification is based on assumption that modal parameters remain constant during a specific time-window where the input-output dataset is analyzed. However, considering that the bridge may enter nonlinear region during large excitation, this assumption may not be satisfied for the whole responses. Therefore, the piecewise linear analysis was conducted on shorter moving time-windows during which the modal parameters were assumed constant. For this reason, the total time history responses were divided into several time windows. Detail information on application of the system identification algorithm to Yokohama-Bay Bridge including numerical simulations to verify its performance under various conditions is given elsewhere [7].

6.2. Observation on modal frequency and damping

Modal frequencies, damping ratios and mode-shapes are identified from MIMO system identification as explained above. Generally, system identification generates 14 modes between 0.1 and 2.5 Hz where the girder modal displacement dominates the mode shapes. Fig.5. illustrates some of mode-shapes identified from 2004 Chuetsu-Niigata earthquake.

Since modal parameters are known to be function of input excitation, the results are evaluated as a function of the Root-Mean-Square (RMS) of the band-pass filtered input acceleration for a particular frequency of interest. Comparisons of the results from earthquakes before 2004, after 2004, and during 2011 Great East-Japan earthquake show that generally natural frequencies decrease with the increase of excitation amplitude [4,7,8]. Larger reductions are observed in natural frequencies of vertical modes than in torsional modes. Damping ratio estimates show large variation within 0.5–6%. In some cases, such as earthquakes before 2004, the result indicates that damping ratios of lower modes increase with the increase of earthquake amplitude [7], which might be due to the results of greater energy dissipation caused by friction in bearings that occurs during large earthquake. However, for the case of larger excitations such as the 2011 Great East-Japan earthquake, the results are quite scattering that drawing a clear relationship between damping ratios and excitation amplitude from such a large scatter estimates becomes difficult.

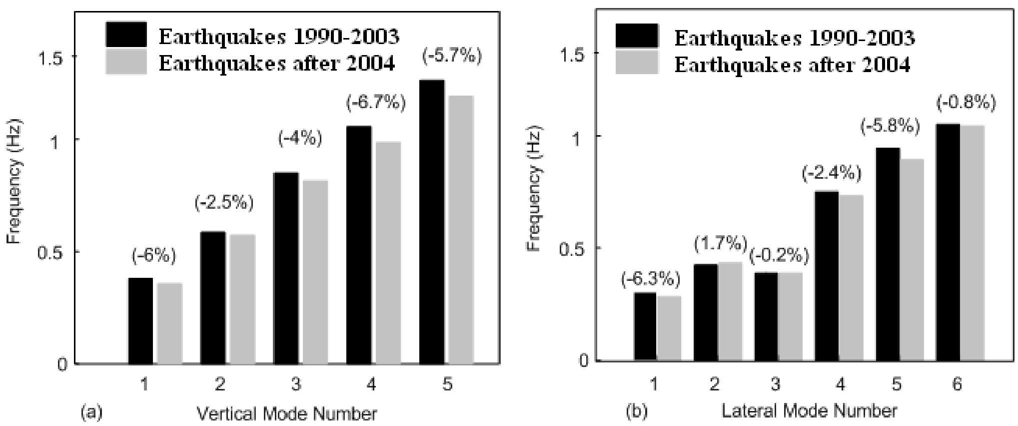

Fig.6. Comparison of natural frequency identified from previous earthquake with the ones identified from the 2004 Chuetsu-Niigata earthquakes and after for (a) vertical mode, (b) Transverse mode. Values in bracket indicate the difference with negative values for decrease.

The frequencies identified from earthquakes on 2004 and after, were lower compared to the corresponding results from earthquakes before 2004 as shown in Fig.6. The decreases in frequencies are between 3 to 7% for vertical modes, 0.8 to 6% for transverse modes and around 3% for torsion modes. These changes are significant and imply that the structural properties may have changed. Considering that the Chuetsu-Niigata earthquake occurred when the construction of additional deck has been completed, the decrease may indicate that the new deck contributes largely as added mass rather than added stiffness to the whole structure system [7].

For the earthquake series related to the 2011 Great East-Japan, it was observed that natural frequencies generally decrease with the increase of excitation amplitude. Larger reductions are observed in natural frequencies of vertical modes than in torsional modes [4]. The most significant reduction is on the second vertical mode (i.e., first asymmetric mode), where the natural frequency decreases from about 0.52–0.55 Hz for input RMS less than 3 cm/s^2 to 0.47 Hz for input RMS of 24 cm/s^2 (about 14% reduction). Damping ratio estimates show large variation within 0.5–6% and drawing a clear relationship between damping ratios and excitation amplitude from such a large scatter estimates is rather difficult.

In general, natural frequencies observed from earthquake records are within good agreement with the results from ambient and forced vibration tests. Most damping ratios are identified with average values in the range of 0.5-6%. This lowest average value (0.5%) is satisfactory according to the minimum damping ratio required by the bridge seismic design and specification. The highest average value (6%), however, is larger than the previously estimated 2% from the study conducted by the Honshu-Shikoku Bridge Authority [8].

6.3. Observation on Link-Bearing performance based on results of system identification

During earthquakes the LBC is designed to function as a perfectly hinged connection along the longitudinal axis. This implies that the girder and pier cap act as separated units and therefore the force from superstructure will not be transmitted to the piers. In designing the end-piers, the assumption of perfectly hinged connection was employed. The actual performance of the LBC is studied by observing modal parameters of the first longitudinal mode identified earthquake records. It should be noted that the longitudinal girder motion induces the nonlinear behavior of the link-bearing connections. This type of motion is excited only by earthquakes and is not measurable during ambient motion measurement and dynamic testing using exciters.

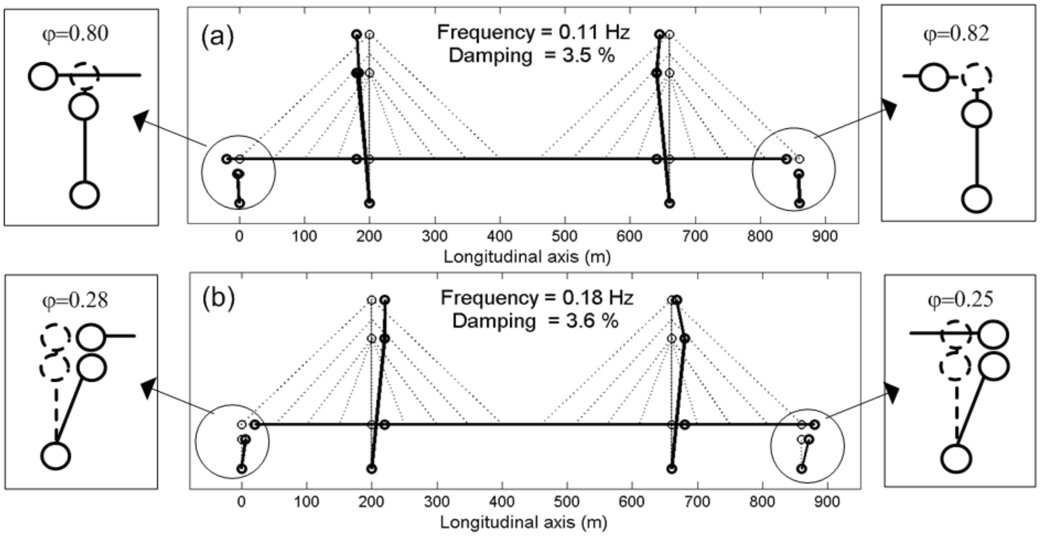

Fig.7 Example of the first longitudinal mode with (a) slip-slip condition and (b) stick-stick condition (After [7]).

Investigation of the LBC is performed by observing the relative modal displacement between pier cap and girder at both end-piers using an index (φ) calculated as $\varphi = \left|(\phi_{girder} - \phi_{pier-cap}) / \phi_{girder}\right|$. The index, ϕ denotes the normalized longitudinal modal displacement of girder, tower and pier at each of LBC location i.e. sensor B3-X and S1-X for P1, sensor T5-X and S3-X for P2, and sensor T6-X and S7-X for P3. To calculate the normalized longitudinal modal displacement, modal displacements at each LBC positions are normalized to maximum value, and then the normalized values are compared to obtain the relative modal displacement between girder and pier cap or between girder and tower at the LBC positions. In case of *slip mode,* φ will be nearly or larger than one whereas for the *stick mode* φ will be closer to zero.

Results for earthquakes from 1990-1997, the 2004 Chuetsu-Niigata and after [7,8], show that there are three typical first longitudinal modes observed. The first mode was identified at around 0.11Hz to 0.15 Hz, which is a typical first mode with the hinge-hinge assumption of end-piers as predicted from the finite element model. This mode exhibits large relative modal displacement between the end-piers cap and the girder, where φ is typically 0.8 or larger or the left and right end-pier respectively. The large gap here suggests that during the earthquake, the fully hinged mechanism at the connection between pier-cap and girder has taken place. The second and third modes were identified at higher frequencies between 0.18 to 0.24 Hz. The second mode exhibits a mixed mechanism in which by judging from the small relative modal displacement, one of the end-pier cap remains fixed or closely connected with the girder, while the other has developed the fully hinged mechanism. This mode typically has φ between 0.5-0.8. In the third mode, an even smaller relative modal displacement between pier cap and girder (φ < 0.5) was observed at the both of end-piers. In this mode, both end-piers cap remain fixed or closely connected to the girder.

In the case of records from 2011 Great East-Japan earthquakes and aftershocks, observation shows that index φ is nearly equal to one suggesting the occurrence of *slip mode*. Furthermore, the occurrence of a *slip mode* indicates an increase in longitudinal flexibility which explains the frequency reduction of longitudinal mode during the largest excitation [4].

It should be mentioned that based on the results of seismic monitoring between 1990 and 2005, it was realized the possibility that LBC may not function properly during a large earthquake. In such a case, excessive moment at the bottom of end-pier may be resulted and the LBCs could fail causing uplift deformation at the girder. As the feedback of the monitoring system, the seismic retrofit of the bridge in 2005 employed a fail-safe design, in which the girder-ends are connected to the footing using prestressed cables to prevent uplift of the girder-end as shown schematically in Fig.8 [1].

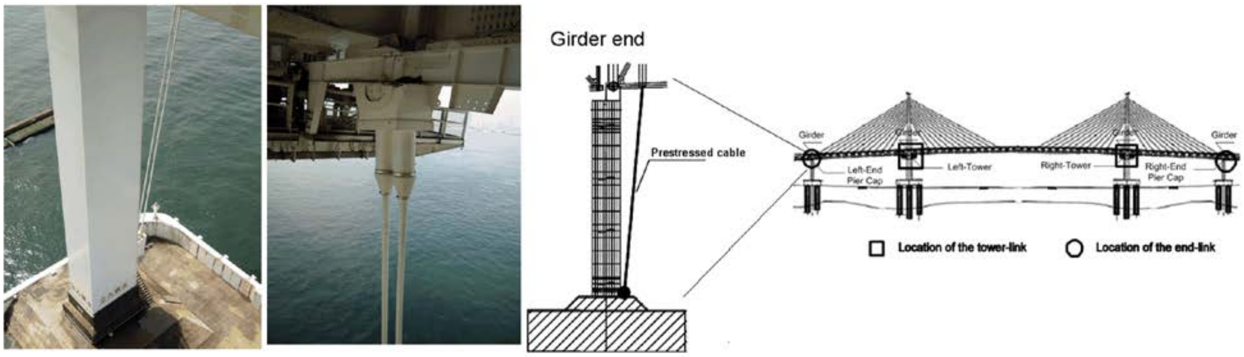

Fig.8. Photos and schematic figure of a fail-safe design system using pre-stressed cable that connects girder-end and the ground to prevent uplift at Yokohama-Bay Bridge

6.4. Observation on Response Nonlinearity and Tower-Girder Transverse Pounding

Indications of responses nonlinearity were observed from the response due to the main shock and the first aftershock of 2011 Great East-Japan earthquake [4]. Results of system identification show that frequency of the first transverse mode increases from 0.27Hz to 0.32Hz during the largest excitation, whereas frequency of the first vertical mode decreases slightly from 0.35Hz to 0.33Hz. The changes in frequencies are followed by the change in transverse-vertical coupling of the girder mode shape. During large excitation, strong coupling is observed in both transverse and vertical modes. The changes in natural frequencies and the transverse-vertical coupling pattern with respect to input amplitude indicate nonlinearity of bridge response. In a subsequent study [9], estimation of damping characteristics of Yokohama-bay Bridge in the nonlinear response range is conducted using a combination of least-square (parametric) and neural network (nonparametric) approaches.

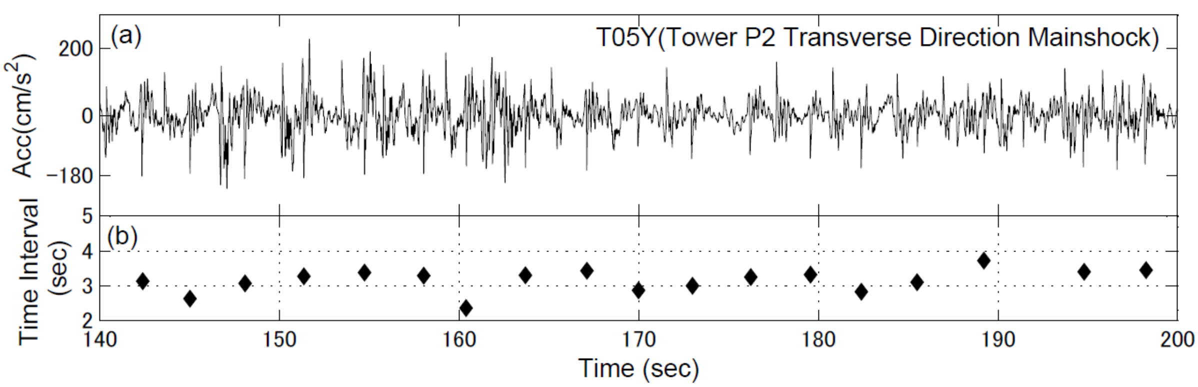

Fig. 9. Close-up look at the tower's transverse (in-plane) acceleration at the tower–girder connections shows periodic impulse response for (a) main shock of 2011 Great East-Japan earthquake and time interval between consecutive impulses

There are several possible sources of nonlinearity in a cable-stayed bridge seismic response, such as material nonlinearity, geometric nonlinearity due to large cable displacement, soil-structure interaction and behavior of pier-girder and tower-girder connections. In the present case, displacement from seismic response was not too large to cause significant geometric or material nonlinear. In addition, tower responses did not show significant indication of non-linearity as expected in a case of significant soil-structure interaction. Considering these conditions, behavior of the tower-girder and the pier-girder connections is thought as a more possible cause of nonlinearity.

Another interesting finding from the records due to the largest ground motion 2011 Great East-Japan earthquake is the indication of tower-girder transverse pounding. The tower transverse accelerations are characterized by many periodic spikes resembling impulses, especially during the largest excitation between 100s and 300s (Fig.9). Periodic impulses indicate occurrence of transverse pounding between tower and girder, and the impulses also appear on the girder vertical accelerations (i.e. sensors S3-Z and S7-Z located above the wind shoes). In addition to the main shock, the same periodic impulses only appear on the tower-girder accelerations during the first aftershock (AS1). By observing time interval between two successive impulses, one can estimate structural mode that triggers the impulse that the girder first transverse mode, since the average time interval between two consecutive impulses is about 3.2 s (0.31- 0.32Hz).

Visual inspection performed afterwards [4]; indicate the occurrence of transverse pounding between girder and tower and the tower-girder connections. Despite its occurrence, transverse pounding did not cause structural damage at the present earthquake. The pounding process is studied using simplified model of two-side contact problem between the nodes that correspond to tower and girder at wind shoes locations [10]. In the model, the values of spring constant that represent the contact stiffness between pier or tower and the girder are determined by adjusting the value of modal parameters identified from seismic response with that of bridge model. The simplified structural model can reasonably simulate the pounding mechanism and its effect on the structure such as the maximum impact force experienced by tower and wind shoes.

7. Serviceability Assessment: Overturned Vehicle Accident

In addition to seismic monitoring system, the bridge is also equipped with traffic monitoring system. During the 2011 Great East-Japan Tohoku Earthquake, the Yokohama Bay Bridge was closed for about 30 hours due to an overturned cargo truck accident on the lower deck as shown in Fig.10. The incident was captured by traffic monitoring system and source of accident has been studied. Preliminary analysis of bridge seismic response and simulation using vehicle shows that in the case of large excitation such as the 2011 Great East-Japan earthquake there exist conditions where the rolling or destabilizing moment acting on vehicle is larger than the resistance moment indicating the onset of vehicle unstable state. This could lead to the rollover condition even when vehicle is moving with constant velocity without driver reaction. The main source of destabilization is reduction of normal force on the wheel due to vehicle's vertical acceleration that offsets the stabilizing gravitational effect. Even if no major structural damage is observed, traffic disruption due to excessive vibration could cause human loss. As wind monitoring data is used to regulate traffic at strong wind conditions, earthquake monitoring and early warning data could also be incorporated into traffic control to reduce this risk.

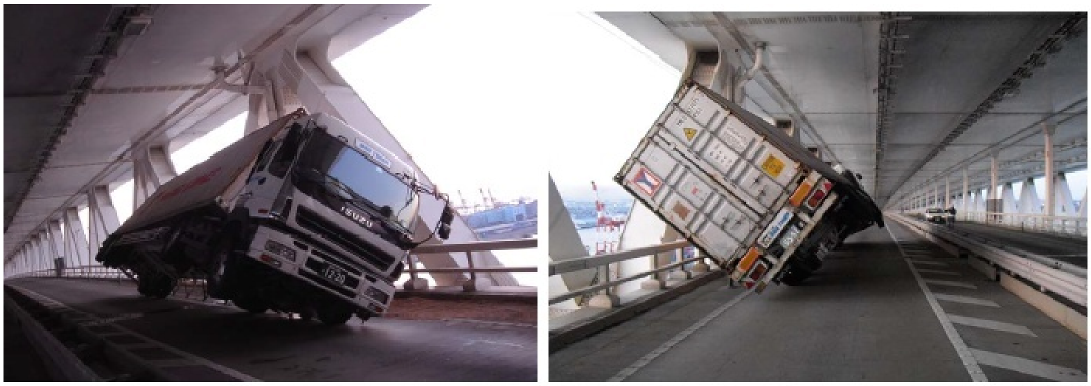

Fig. 10. Photos of rollover incident of a cargo truck on the lower deck of Yokohama-Bay Bridge taken from closed-circuit TV camera during the March 11, 2011 Great East Japan Earthquake

8. Conclusions

This paper describes an overview of seismic monitoring of Yokohama-Bay cable-stayed bridge and the lessons learned from monitoring results for over twenty years. Structural responses of the bridge from more than one hundred earthquake events between 1990 and 2011 have been recorded, with the largest one being the 2011 Great East-Japan earthquake. Using data monitoring system and by employing relevant methodologies on system identification and structural analysis various structural aspects such as modal characteristics and their dependency on excitation level, performance of seismic isolation system, response nonlinearity and structural pounding were analyzed.

The study demonstrates that permanent seismic monitoring provides indispensible data of structure behavior during under various levels of earthquake. They have been shown to be particularly useful for understanding of real structural behaviors in depth, revealing unknown factors that were not considered in design such as the unanticipated variation of LBC performance and transverse structural pounding, and providing structural information for necessary retrofit after extreme events.

9. Acknowledgement

The authors gratefully acknowledge Metropolitan Expressway Public Corporation, Tokyo, Japan, especially Mr. Kenji Namikawa for collaboration in this study and for access to the seismic monitoring system. Valuable discussion with Dr. Masaaki Yabe of Chodai Consulting Engineering is also highly appreciated. This study is supported by JSPS through Grant-in-Aid for Encouragement of Young Scientists (B) No. 15K18104 to the first author. This support is gratefully acknowledged.

10. References

[1] Fujino Y, Siringoringo, DM (2011): Bridge monitoring in Japan: the needs and strategies. *Structure and Infrastructure Engineering*, **7**(7-8), 597-611.

[2] Maeda K, Otsuka A, Takano H. (1991): The design and construction of Yokohama Bay Bridge, *Cable-Stayed Bridges Recent Developments and their Futures, M.Ito et.al. (Editors).* Elsevier Science Publisher B.V., 377-395.

[3] The Metropolitan Expressway Public Corporation (1991): The Yokohama Bay Bridge, Tokyo Japan, 164-172 (in Japanese).

[4] Siringoringo DM, Fujino Y, Namikawa K (2013): Seismic response analyses of the Yokohama Bay cable-stayed bridge in the 2011 great East Japan earthquake. *Journal of Bridge Engineering ASCE*, **19**(8), A4014006,1-17.

[5] Fujino Y, Kikkawa H, Namikawa K, Mizoguchi T (2005): Seismic Retrofit Design of Long-Span Bridges on Metropolitan Expressways in Tokyo. *Proc. of the 6th Intl. Bridge Eng. Conf. Transportation Research Board*, Boston Mass, USA, CD-ROM.

[6] Juang JN, (1997). System Realization Using Information Matrix. *J. Guidance, Control, and Dynamics*, **20**(3), 492-500.

[7] Siringoringo DM, Fujino Y (2008): System identification applied to long-span cable-supported bridges using seismic records. *Earthquake Engineering & Structural Dynamics*, **37**(3), 361-386.

[8] Siringoringo DM, Fujino Y (2006): Observed dynamic performance of the Yokohama-Bay Bridge from system identification using seismic records. *Structural Control and Health Monitoring*, **13**(1), 226-244.

[9] Derkevorkian A, Masri SF, Fujino Y, Siringoringo DM (2014): Development and validation of nonlinear computational models of dispersed structures under strong earthquake excitation. *Earthquake Engineering & Structural Dynamics*, **43**(7), 1089-1105.

[10] Siringoringo DM, Takamoto G, Fujino Y (2015): Analysis of Tower-Girder Transfer Pounding on the Yokohama-Bay Cable-Stayed Bridge during 2011 Great East Japan Earthquake. *IABSE Symposium Report* , **104**(1), 1-8.